

Open Research Online

The Open University's repository of research publications and other research outputs

ISO observations of the HH 24-26 regions

Conference or Workshop Item

How to cite:

Benedettini, M.; Giannini, T.; Nisini, B.; Tommasi, E.; di Giorgio, A. M.; Lorenzetti, D.; Saraceno, P.; Smith, H. A. and White, G. J. (1999). ISO observations of the HH 24-26 regions. In: The Universe as Seen by ISO, 20-23 Oct 1998, Paris, p. 471.

For guidance on citations see [FAQs](#).

© Journal

Version: Version of Record

Link(s) to article on publisher's website:

<http://adsabs.harvard.edu/abs/1999ESASP.427..471B>

Copyright and Moral Rights for the articles on this site are retained by the individual authors and/or other copyright owners. For more information on Open Research Online's [data policy](#) on reuse of materials please consult the policies page.

oro.open.ac.uk

ISO OBSERVATIONS OF THE HH 24-26 REGION

M. Benedettini¹, T. Giannini^{1,2,3}, B. Nisini¹, E. Tommasi⁴,
A.M. Di Giorgio¹, D. Lorenzetti², P. Saraceno¹, H.A. Smith⁵, G.J. White⁶

¹CNR-Istituto di Fisica dello Spazio Interplanetario, Roma, Italy

²Osservatorio Astronomico di Roma, Monte Porzio, Italy

³Università La Sapienza, Roma, Italy

⁴Agenzia Spaziale Italiana, Roma, Italy

⁵Harvard - Smithsonian Center for Astrophysics, Cambridge, MA, USA

⁶Queen Mary & Westfield College, London, UK

ABSTRACT

We report the results of an investigation, performed with the Long Wavelength Spectrometer (LWS) and the Short Wavelength Spectrometer (SWS) on-board the ISO satellite, on the star forming region associated with the Herbig-Haro objects HH24-25 and 26. In particular, we obtained low-resolution LWS spectra towards the two Class 0 sources HH24MMS and HH25MMS as well as towards the Class I source HH26IR and its associated flow. In addition, SWS scans of pure H₂ rotational lines in HH24MMS were acquired.

All the spectra present the [OI] 63 μm and the [CII] 158 μm lines, while significant molecular emission from CO and H₂O is detected only from HH25MMS and along the blue lobe of the HH26IR outflow, where the shocked activity is also evidenced by the presence of strong near infrared knots. The physical conditions of the regions strongly emitting in molecular lines are derived, showing that the two Class 0 sources are characterised by lower temperatures and higher densities than the HH26IR flow. The presence of both J and C shocks are envisaged to take into account the observed emission.

Key words: ISM; infrared lines; Herbig-Haro objects.

1. INTRODUCTION

The Herbig-Haro (HH) objects HH24-25 and 26 are located within the L1630 dark cloud (distance ~ 400 pc, Anthony-Twarog 1982), few arcminutes south of NGC2068. Their associated star forming region has a complex morphology where young sources of different evolutionary stage are present together with their associated outflows. HH24 and 25 are excited by two very young Class 0 sources (HH24MMS and HH25MMS) located within two dense molecular cores (Davis et al. 1997, Bontemps, André and Ward-Thompson 1995). Each of these sources is also

driving a compact jet traced by means of the 2.12 μm H₂ line and CO mm observations (Gibb & Davis 1998, Bontemps et al. 1996). HH26 is associated with an apparently more evolved (Class I) source, HH26IR, which drives an extended molecular outflow (Gibb & Heaton 1993) also traced by the 2.12 μm H₂ line (Davis et al. 1997). In the region also four low luminosity IRAS sources are present, which however do not seem to be connected with the HH objects and the different outflow activities.

Here we present the results of a spectroscopic investigation performed with ISO, with the aim of studying the far-infrared cooling due to atoms, like O^o and molecules, like CO and H₂O, which are expected to copiously emit in the excitation conditions prevailing in star forming regions.

2. OBSERVATIONS

Spectra from 43 to 197 μm have been acquired with LWS (Clegg et al. 1996) in the low-resolution mode (resolution ~ 200); the spectra are oversampled by a factor 4. Raw data have been reduced with the Off-Line Processing (OLP) version 7. In Table 1 we present the Journal of observations. For HH24MMS and HH25MMS, the LWS beam of ~ 75 arcsec encompasses the MM source as well as the associated HH and jet, while HH26IR and the associated outflow have been mapped by means of three different observations partially overlapping. Only on HH24MMS, H₂ pure rotational lines ($\nu=0\rightarrow 0$) from S(1) to S(5) have been scanned with SWS (de Graauw et al. 1996) in the AOT02 mode (resolution ~ 1200 , beam size 14×20 arcsec², total integration time 200 sec) and the raw data have been processed with the OLP version 6. Both SWS and LWS data have been cleaned from spurious signals due to cosmic ray impact; in addition, for the LWS data we have averaged together the scans of each detector and removed the interference fringes, while for the SWS scans the 12 detectors have been averaged, rebinning the data at twice the instrumental resolution.

Table 1. Journal of observations.

Source	Date	rev.		α	(2000)	δ	(2000)	t_{int}	n_s	
			h	m	s	°	'	''	sec	
HH24MMS SWS	14 Oct 97	698	5	46	08.6	-0	10	40.8	-	-
HH24MMS	14 Oct 97	698	5	46	08.6	-0	10	40.8	10	25
HH25MMS	10 Oct 97	694	5	46	06.7	-0	13	24.7	10	25
HH26blue	10 Oct 97	694	5	46	08.9	-0	14	26.8	4.8	12
HH26IR	10 Oct 97	694	5	46	03.9	-0	14	52.5	4.8	12
HH26red	10 Oct 97	694	5	46	01.6	-0	15	23.3	4.8	12

Notes: rev. = revolution, t_{int} =integration time per spectral sample; n_s = number of spectral scans.

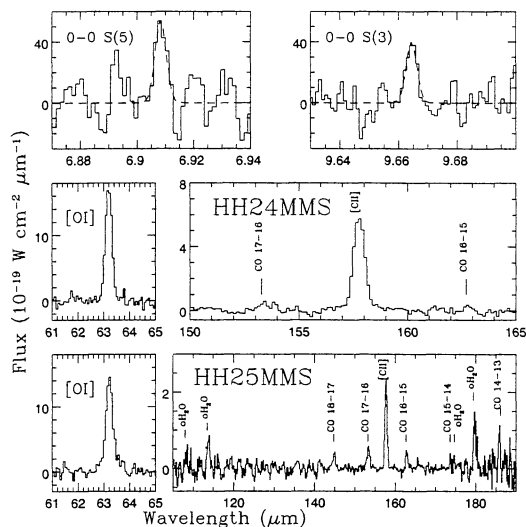


Figure 1. The two upper plots show the SWS H_2 scans on HH24MMS, while the middle and lower plots show the continuum subtracted portions of LWS spectra for HH24MMS and HH25MMS respectively.

3. RESULTS AND DATA ANALYSIS

The SWS data on HH24MMS show a signal to noise ratio greater than 3 only for the S(3) and S(5) lines. All the LWS spectra present the [OI] 63 μ m and the [CII] 158 μ m atomic lines. High-J CO transitions are observed in all the targeted positions but HH26red, while o- H_2O emission is detected only on HH25MMS and along the blue lobe of the HH26IR outflow. In particular the molecular lines we find are: on HH24MMS the $J_{up}=17$ CO line; on HH25MMS the CO lines from $J_{up}=14$ to $J_{up}=18$ and three o- H_2O lines, namely $4_{14}-3_{03}$ (113.5 μ m), $3_{03}-2_{12}$ (174.6 μ m) and $2_{12}-1_{01}$ (179.5 μ m); on HH26blue the CO lines from $J_{up}=16$ to $J_{up}=20$ and the o- H_2O transition $4_{14}-3_{03}$ and on HH26IR the CO lines from $J_{up}=16$ to $J_{up}=18$. The portions of the spectra in which the lines are observed are shown in Figures 1 and 2.

The CO and o- H_2O emission lines have been used to fit the temperature and the density of the emitting region by means of a model which solve the equations of

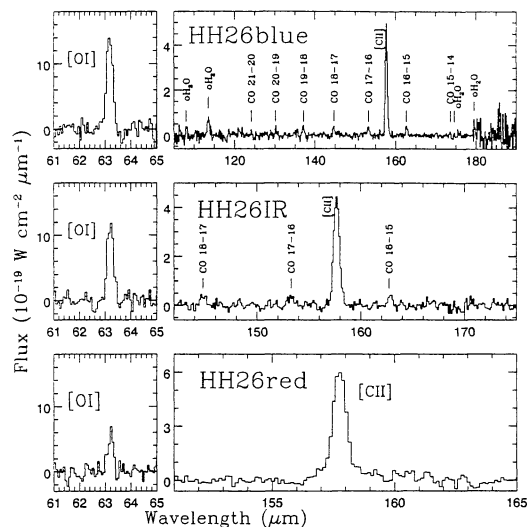


Figure 2. Continuum subtracted LWS spectra of HH26blue, HH26IR and HH26red

the statistical equilibrium for the level populations by using a Large Velocity Gradient (LVG) approximation in plane-parallel geometry (Giannini et al. 1998, Nisini et al. 1999). We assume that all the molecular components are originated in the same region. In Table 2 we summarize the physical parameters derived from this analysis, namely temperature, density and line cooling. In this table we also report the mass loss rate (\dot{M}) derived from the [OI]63 μ m luminosity under the assumption that this line is emitted from the shock due to the interaction of the stellar wind with the ambient medium (Hollenbach 1985); for comparison, we also give the kinetic luminosity and \dot{M}_w of the outflows derived from the CO maps (Gibb & Heaton 1993, Gibb & Davis 1998). In the following, a description of the results obtained from each source is given.

3.1. HH25MMS

From the detected CO molecular lines we derive quite stringent temperature and density estimations: $T=300\div 550$ K and $n_{H_2}=5\cdot 10^5\div 10^6$ cm^{-3} respec-

Table 2. Physical parameters.

	HH24MMS	HH25MMS	HH26blue
T (K)	450±50	300-550	~1800
n_{H_2} (cm^{-3})	>10 ⁶	(0.5-1)10 ⁶	~1.6·10 ⁻⁴
$L_{[OI]}$ (L_{\odot})	0.027	0.024	0.022
molecular cooling (L_{\odot})	0.022	0.12	0.14
kinetic luminosity (L_{\odot}) *	-	> 0.007	0.16
$\dot{M}_w([OI]63 \mu\text{m})$ ($M_{\odot} \text{ yr}^{-1}$)	(2.6±0.1)10 ⁻⁶	(2.28±0.09)10 ⁻⁶	(2.1±0.1)10 ⁻⁶
$\dot{M}_w(\text{outflow})$ ($M_{\odot} \text{ yr}^{-1}$) *	-	>6.4·10 ⁻⁸	1.8·10 ⁻⁶

* From CO mm observations (see text).

tively. In Figure 3 we show the model fit to the CO data. The three o-H₂O detected lines are all the backbone lines below the 4₁₄ energy level and their fluxes are consistent with the physical conditions derived from the CO line fitting. The cooling due to all the emitted lines (CO, o-H₂O, [OI] and H₂ taken from Davis et al. 1997) is 0.14 L_{\odot} and the $\dot{M}_w([OI]63 \mu\text{m})=(2.28\pm 0.09)10^{-6}M_{\odot}\text{yr}^{-1}$. These values are higher than those estimated from mm CO observations (Gibb & Davis 1998), which could indicate a source of excitation for the FIR lines in addition to the outflow; the outflow parameters are however only lower limits to the true values, due to both the incomplete mapping of the flow and its high inclination with respect to the line of sight which would need a large correction to the flow velocity, not taken into account in the values derived by Gibb and Davis (1998).

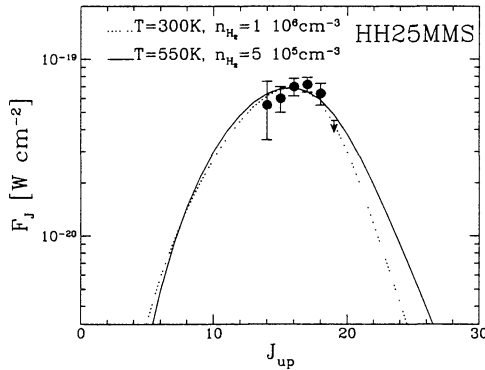


Figure 3. Observed CO line fluxes in HH25MMS and model fits compatible with the data.

3.2. HH26IR AND ITS OUTFLOW

For the blue lobe of the outflow (HH26blue) we can give only a rough estimate of the gas temperature and density from the analysis of the CO lines, *i.e.* $T=400\div 1800$ K and $n_{H_2}=1.6\cdot 10^4\div 2\cdot 10^6$ cm^{-3} respectively. However, in Figure 5 it is shown that the ratio between the upper limit of the 2₂₁-1₁₀ (108.1 μm) and the 4₁₄-3₀₃ (113.5 μm) o-H₂O lines rules out lower temperature and higher density models.

The three CO lines detected on HH26IR, are not sufficient to constrain the local physical parameters by using our LVG model. However, comparing the HH26IR CO lines with those observed on HH26blue we note that they have the same line ratio; considering that the two observations partially overlap, we can suppose that in the on-source measure we are detecting part of the CO emission present in the blue lobe of the outflow.

On the red lobe of the outflow (HH26red) we do not detect any molecular line. Along the outflow both the molecular and the [OI]63 μm emission seem to be correlated with the H₂ 2.12 μm emission (Fig. 6 and Table 1 in Davis et al. 1997). This indicates that also the FIR emission is likely due to shock excitation; moreover, this also shows that the excitation in the red lobe is really lower than in the blue lobe and that the lower H₂ luminosity in this part of the flow is not due only to a larger reddening. The connection of the observed emission with the outflow activity is also demonstrated by the agreement of the $\dot{M}_w([OI]63 \mu\text{m})$ with the corresponding value derived from mm observations (Gibb & Heaton 1993), and by the equality between the total line cooling and the kinetic luminosity of the flow, as expected in jet-driven molecular outflows models (Davis and Eisloffel 1996).

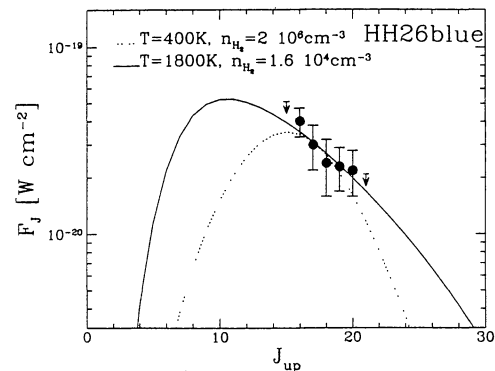


Figure 4. Observed CO line fluxes in HH26blue and model fits compatible with the data.

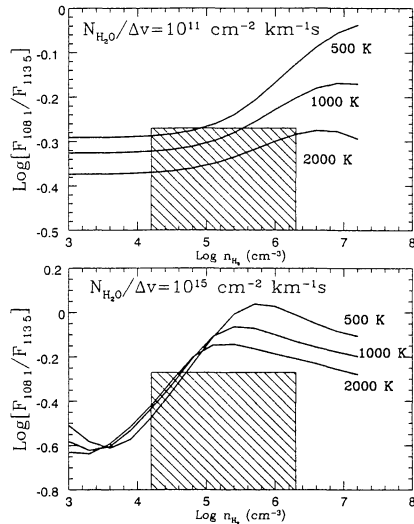


Figure 5. The 108.1 $\mu\text{m}/113.5 \mu\text{m}$ water lines ratio vs gas density for three temperatures (500, 1000, 2000 K) and for two values of $N_{\text{H}_2\text{O}}/\Delta v$, as predicted by the LVG model. The dashed region is limited by the density range derived from CO line fitting and the upper limit ratio obtained on HH26blue.

3.3. HH24MMS

From the ratio of the two H_2 rotational lines we derive a gas temperature of 450 ± 50 K. With this temperature, if we assume that the only CO detected line ($J_{up}=17$) is the most luminous CO line, as supported by the fact that the adjacent lines have smaller flux upper limits, we can derive a gas density between 10^6 and 10^7 cm^{-3} , in agreement with the estimate of Gibb & Heaton (1993) of $n_{\text{H}_2} > 10^6 \text{ cm}^{-3}$ for the dense core where HH24MMS is located. The line cooling is $0.16 L_{\odot}$ and the $\dot{M}_w([\text{OI}]63 \mu\text{m}) = (2.6 \pm 0.1) 10^{-6} M_{\odot} \text{ yr}^{-1}$, which however cannot be compared with the corresponding values from mm observations.

4. GENERAL CONCLUSIONS

The analysis of the FIR molecular lines indicates that the HH26IR flow is characterised by lower densities and higher temperatures than the two Class 0 sources HH24MMS and HH25MMS. This is confirmed by the CS and HCO^+ maps (Gibb & Heaton 1993) showing that HH24MMS and HH25MMS are located in dense clumps ($n_{\text{H}_2} > 10^5 \text{ cm}^{-3}$), while the entire HH26IR flow is not associated with any density peak.

The observed [CII] line intensity is not correlated with the presence of the infrared sources in the investigated fields (see Figure 6), excluding the occurrence of strong PDR excitation related to these sources.

We have shown that the [OI]63 μm and molecular emission are certainly due to shock excitation at

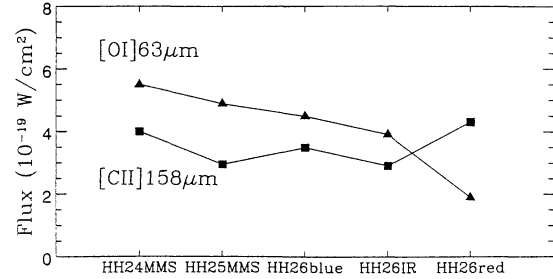


Figure 6. Line fluxes of [OI]63 μm and [CII]158 μm measured in the observed positions.

least for the HH26IR outflow; for HH25MMS and HH24MMS, shocks remain the most natural source of excitation even if the evidences are not so compelling. The correlation of the [OI]63 μm luminosity with the outflow mass loss rate for the HH26IR flow indicates the presence of dissociative J-shocks as expected for a region where the HH objects are travelling at more than 100 km s^{-1} . On the other hand, both the strong NIR (H_2) and FIR (CO and H_2O) molecular emission, whose total cooling is exceeding the contribution due to the [OI]63 μm emission, indicate that also lower velocity non-dissociative shocks (C-shocks) may contribute to the gas excitation of HH25MMS and HH26blue.

REFERENCES

- Anthony-Twarog, B.J. 1982, AJ, 87, 1213
 Clegg, P.E., Ade, P.A.R., Armand, C., et al. 1996, A&A, 315, L38
 Bontemps, S., André, P., Ward-Thompson, D. 1995, A&A, 297, 98.
 Bontemps, S., Ward-Thompson, D., André, P. 1996, A&A, 314, 477
 Davis, C.J., Ray, T.P., Eisloffel, J., Corcoran, D. 1997, A&A, 324, 263.
 Davis, C.J., Eisloffel 1996, A&A, 300, 851
 de Graauw, T., Haser, L.N., Beintema, D.A. et al. 1996, A&A, 315, L49
 Giannini, T., Lorenzetti, D., Tommasi, E. et al. 1998, A&A, submitted
 Gibb, A.G., Heaton, B.D. 1993, A&A, 276, 511
 Gibb, A.G., Davis, C.J. 1998, MNRAS, 298, 644
 Nisini, B., Benedettini, M., Giannini, T., et al. 1999, in preparation
 Hollenbach, D.J. 1985 Icarus, 61, 40